

AD-752 603

EVALUATION OF TEST DATA ON JET ENGINE
COMBUSTOR BURN-THROUGH FLAMES

H. S. Pergament, et al

AeroChem Research Laboratories, Incorporated

Prepared for:

National Aviation Facilities Experimental Center

March 1972

DISTRIBUTED BY:

NTIS

National Technical Information Service
U. S. DEPARTMENT OF COMMERCE
5285 Port Royal Road, Springfield Va. 22151

EVALUATION OF TEST DATA ON JET ENGINE COMBUSTOR BURN-THROUGH FLAMES

AD 752603

H. S. Pergament & R. R. Mikatarian
AeroChem Research Laboratories, Inc.
Sybron Corporation
Princeton, New Jersey 08540



transpo
U.S. International Transportation Exposition
Dulles International Airport
Washington, D.C.
May 27-June 4, 1972

MARCH 1972

FINAL REPORT

Availability is unlimited. Document may be released to the National Technical Information Service, Springfield, Virginia 22151, for sale to the public.

Reproduced by
NATIONAL TECHNICAL
INFORMATION SERVICE
U.S. Department of Commerce
Springfield VA 22151

Prepared for

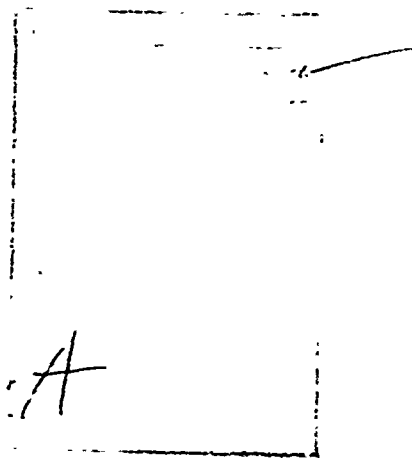
DEPARTMENT OF TRANSPORTATION
FEDERAL AVIATION ADMINISTRATION
Systems Research & Development Service
Washington D. C., 20591

18
P

REVERSE OF COVER

The contents of this report reflect the views of the contractor, which is responsible for the facts and the accuracy of the data presented herein, and do not necessarily reflect the official views or policy of the FAA or Department of Transportation. This report does not constitute a standard, specification, or regulation.

The Federal Aviation Administration is responsible for the promotion, regulation and safety of civil aviation and for the development and operation of a common system of air navigation and air traffic control facilities which provides for the safe and efficient use of airspace by both civil and military aircraft.



1. Report No. FAA-RD-71-100		2. Government Accession No.		3. Recipient's Catalog No.	
4. Title and Subtitle EVALUATION OF TEST DATA ON JET ENGINE COMBUSTOR BURN-THROUGH FLAMES				5. Report Date March 1972	
				6. Performing Organization Code	
7. Author(s) H.S. Pergament R.R. Mikatarian				8. Performing Organization Report No. AeroChem TP-261 FAA-NA-72-30	
9. Performing Organization Name and Address AeroChem Research Laboratories, Inc. Sybron Corporation P.O. Box 12 Princeton, New Jersey 08540				10. Work Unit No.	
				11. Contract or Grant No. DOT-FA71NA-575	
12. Sponsoring Agency Name and Address Federal Aviation Administration Systems Research & Development Service Washington, D.C. 20591				13. Type of Report and Period Covered Final Report 4 May - 4 July 1971	
				14. Sponsoring Agency Code	
15. Supplementary Notes This study was made under a contract administered by the National Aviation Facilities Experimental Center, Atlantic City, N.J.					
16. Abstract A method is developed to interpret flat plate impingement pressure and temperature data taken in jet engine combustor burn-through flames in terms of free stream velocities, pressures, temperatures, etc. These flames, which are high-temperature, turbulent, underexpanded sonic jets, are caused, in practice, by the combustion gases impinging on (and burning a hole through) the wall of the combustor. The free stream property data are needed to compute local heat transfer coefficients, which must be known to determine whether potential firewall materials can withstand a burn-through flame. Turbulent convective heat transfer coefficients are computed herein, primarily to determine radiation and conduction corrections to the temperature measurements. The influence of mixing between the burn-through flame and ambient air on flame properties is also studied, and a correlation is developed which relates the angle of spread of the mixing region to the enthalpy flux at the burn-through hole. Suggestions regarding future experimental and theoretical programs are made.					
17. Key Words Jet engine combustors Burn-through flames Turbulent supersonic jets Turbulent heat transfer to flat plates				18. Distribution Statement Availability is unlimited. Document may be released to the National Technical Information Service, Springfield, Virginia 22151, for sale to the public.	
19. Security Classif. (of this report) Unclassified		20. Security Classif. (of this page) Unclassified		21. No. of Pages 48	22. Price \$3.00

PREFACE

This report was prepared by AeroChem Research Laboratories, Inc., Princeton, New Jersey for the Federal Aviation Administration. The work was administered under the direction of Mr. Thomas Rust, Jr., Project Manager, Propulsion Section, Aircraft Branch, National Aviation Facilities Experimental Center, (NAFEC) Atlantic City, New Jersey.

TABLE OF CONTENTS

	<u>Page</u>
INTRODUCTION	1
Purpose	1
Background	1
DISCUSSION	2
Interpretation of Flat Plate Pressure Data	2
Shock Locations	2
Flat Plate Normal Shock Corrections	3
Mach Number and Pressure Distributions	4
Velocity Distributions	6
Thermocouple Corrections	7
Radiation	7
Conduction	9
Mass Flow Rates	10
Influence of Mixing on Flame Properties	10
Suggested Experimental Methods for Future Test Programs	12
Burn-Through Flame Properties	12
Photographs	12
Sampling	13
Effects of Noncircular Holes	13
Heat Transfer Coefficients	13
CONCLUSION	15
APPENDIX A	1-1
Figures Evolving from the Study of Test Data on Jet Engine Combustor Burn-Through Flames (15 pages)	
APPENDIX B	2-1
Tables Pertinent to the Study of Test Data on Jet Engine Combustor Burn-Through Flames (8 pages)	
APPENDIX C	3-1
References (2 pages)	

LIST OF ILLUSTRATIONS

<u>Figure</u>		<u>Page</u>
1	COMPARISON BETWEEN SHOCK LOCATIONS IN NAFEC TESTS AND UNDEREXPANDED AIR JET DATA	1-3
2	RELATIVE POSITIONS OF SHOCKS UPSTREAM OF A FLAT PLATE AND A PITO TUBE	1-4
3	EFFECT OF MACH NUMBER ON SHOCK DETACHMENT DISTANCE FROM FLAT PLATE	1-5
4a	PROPERTY DISTRIBUTIONS ALONG CENTERLINE OF BURN-THROUGH FLAME (95% power setting)	1-6
4b	PROPERTY DISTRIBUTIONS ALONG CENTERLINE OF BURN-THROUGH FLAME (90% power setting)	1-7
4c	PROPERTY DISTRIBUTIONS ALONG CENTERLINE OF BURN-THROUGH FLAME (85% power setting)	1-8
4d	PROPERTY DISTRIBUTIONS ALONG CENTERLINE OF BURN-THROUGH FLAME (80% power setting)	1-9
4e	PROPERTY DISTRIBUTIONS ALONG CENTERLINE OF BURN-THROUGH FLAME (75% power setting)	1-10
4f	PROPERTY DISTRIBUTIONS ALONG CENTERLINE OF BURN-THROUGH FLAME (70% power setting)	1-11
4g	PROPERTY DISTRIBUTIONS ALONG CENTERLINE OF BURN-THROUGH FLAME (60% power setting)	1-12
4h	PROPERTY DISTRIBUTIONS ALONG CENTERLINE OF BURN-THROUGH FLAME (50% power setting)	1-13
5	EFFECT OF ENGINE POWER SETTING ON CENTERLINE STAGNATION ENTHALPY DISTRIBUTIONS	1-14
6	INFLUENCE OF BURN-THROUGH FLAME ENTHALPY FLUX ON MIXING CORE LENGTH	1-15

LIST OF TABLES

<u>Table</u>		<u>Page</u>
1	PROPERTIES IN COMBUSTOR	2-3
2	FLAT PLATE IMPINGEMENT PRESSURES	2-4
3	UNCORRECTED FLAT PLATE THERMOCOUPLE READINGS	2-5
4	STAGNATION TEMPERATURES ON BURN-THROUGH FLAME CENTERLINE	2-6
5	MASS FLOW RATES	2-7
6	LENGTH OF CORE REGION	2-8

LIST OF SYMBOLS

A_{ex}	area of burn-through hole
A_j	area of thermocouple junction
A_w	cross sectional area of thermocouple wire
a	speed of sound
c_p	specific heat at constant pressure
c_{pD}	specific heat of calorimeter disc
d	burn-through hole diameter ($d = 1$ inch in this report)
$(dT/ds)_j$	temperature gradient at thermocouple junction
E	enthalpy flux at burn-through hole
H_{amb}	stagnation enthalpy at ambient temperature
H_o	local stagnation enthalpy in jet
H_{oc}	stagnation enthalpy at combustor temperature
h	convective heat transfer coefficient
h_{turb}	turbulent heat transfer coefficient
k	thermal conductivity of gas
k_p	thermal conductivity of plug
k_w	thermal conductivity of thermocouple wire
m_D	mass of calorimeter disc
M_{ex}	Mach number at burn-through hole
M_{plate}	free stream Mach number upstream of flat plate normal shock
M_{probe}	free stream Mach number upstream of probe normal shock
M_1	free stream Mach number immediately upstream of normal shock
$M_1^{(0)}$	free stream Mach number immediately upstream of oblique shock
M_2	Mach number immediately downstream of normal shock
$M_2^{(0)}$	Mach number immediately downstream of oblique shock
M_∞	free stream Mach number
Nu	Nusselt number, $Nu = hd/k$

P_0	stagnation pressure
P_{O_2}	stagnation pressure downstream of shock
P_{OFP}	flat plate impingement pressure
Pr	Prandtl number, $Pr = \mu c_p/k$
p	static pressure
P_{ex}	static pressure at burn-through hole
P_1	static pressure upstream of normal shock
P_∞	ambient pressure
P_2	static pressure downstream of normal shock
q_{cond}	conductive heat transfer rate
q_{conv}	convective heat transfer rate
R	gas constant (53.3 ft-lb _f /lb _m -°R)
Re	Reynold's number, $Re = \frac{\rho u d}{\mu}$
s	distance along thermocouple wire
T	static temperature
T_{amb}	ambient temperature
T_{ex}	temperature at burn-through hole
T_i	initial temperature of plug (at $t = 0$)
T_0	stagnation temperature
T_p	temperature of plug exposed to burn-through flame
T_w	thermocouple junction temperature
T_2	static temperature downstream of normal shock
t	time
u	velocity
u_{ex}	velocity at burn-through hole
u_2	velocity downstream of normal shock
w	mass flow rate
x	axial distance from burn-through hole
y	distance normal to flame axis

Greek

α	thermal diffusivity of plug
γ	ratio of specific heats
Δ	shock detachment distance
ϵ	emissivity
ρ_{ex}	density at burn-through hole
ρ_2	gas density downstream of normal shock
σ	Stefan-Boltzmann constant, $\sigma = 1.73 \times 10^{-9}$ Btu/hr-ft ² - (°R) ⁴
μ_2	viscosity of gas downstream of normal shock
θ	angle of spread of mixing region, $\theta = \tan^{-1} d/2L$

Miscellaneous

erfc complementary error function, $\text{erfc}(X) = \frac{2}{\sqrt{\pi}} \int_X^{\infty} e^{-\lambda^2} d\lambda$

INTRODUCTION

Purpose

It is the purpose of this study to utilize existing theory and data on supersonic flows similar to jet engine combustor burn-through flames, along with the measured flat plate impingement pressure and temperatures of Ref. 1 to determine inter alia the distributions of velocity, Mach number, pressure and stagnation temperature (corrected for radiation and conduction errors) along the flame centerline.

Background

Considerable background on the problem of jet engine combustor burn-through failures is given by Rust,¹ who gives the following description of a burn-through:

"A burn-through occurs in an engine when the hot combustion gases within a combustion chamber are deflected from their normal path and impinge on the wall of the combustion chamber, thus causing a hot spot on the wall. The heat on the wall weakens it, and the high pressure in the chamber causes a bursting type failure at this point. The result is a severe high temperature, high velocity flame escaping from the hole in the chamber."

In Ref. 1, the results of an experimental study of a burn-through flame on a J47-GE-25 jet engine combustor are presented. In this investigation the flame was simulated by (1) making an irregularly shaped hole in the flame tube which fits inside the burner can, (2) inserting a baffle plate between the flame tube and the burner can--creating a low pressure region aft of the baffle plate--causing the flame to impinge on the burner-can wall, and (3) making a 1-in. -diameter hole at the impingement point, allowing the combustion gases to exhaust to atmospheric pressure.

A number of candidate firewall* materials were placed in the flame to determine how long they could withstand the severe heating conditions. In addition, plate impingement pressure and stagnation temperature were measured in an attempt to determine the pertinent flame properties; e. g. , temperature, pressure, velocity, etc. These measurements were made with a pitot pressure-measuring hole and a thermocouple inserted at the center of a flat plate, positioned normal to the flow. Measurements were made on the flame centerline at various axial distances from the burn-through hole. Although the above measurements gave the pressure and temperature experienced by a firewall material in the flame, additional interpretation of the data is required to determine local flame properties.

* The firewall is used to protect other parts of the aircraft from a burn-through flame.

In the discussion part of this report, a technique for interpretation of the pressure data in terms of the local flame centerline properties is described. This is followed by a description of a method for computing the convective heat transfer coefficients needed as input data for the thermocouple radiation and conduction corrections. Discussed next are the effects of mixing between the flame and ambient air on the centerline properties. Finally recommendations are presented regarding instrumentation and data interpretation for future test programs to be carried out at NAFEC, similar in nature to the program described in Ref. 1. (All references are in Appendix C.)

DISCUSSION

Interpretation of Flat Plate Pressure Data

If the ratio of stagnation pressure in the combustor to ambient pressure is greater than about 1.8 (for $\gamma = 1.3$),* the flow will be sonic at the burn-through hole. Table 1 (All tables are in Appendix B.) gives the properties in the combustor and at the hole, and indicates that $M_{ex} = 1$ for all power settings, except 50 percent. It is noted that for power settings ≥ 70 percent the pressure at the hole is greater than 1 atmosphere (atm); thus, the burn-through flame is actually a high-temperature, underexpanded sonic jet.

Shock Locations: In order to gain confidence in the subsequent analysis of flame properties, shock locations obtained from flame photos for the 80 percent and 90 percent power settings[†] were compared with data available in the literature^{2,3} on underexpanded sonic air jets. The results of this comparison are given in Fig. 1. (All illustrations are in Appendix A.) It can be seen that all data on first shock locations are consistent, and a smooth curve can readily be drawn through all the points. NAFEC data¹ on the other shock locations are seen to be consistent with the ARAP data.² Figure 1 was used to determine shock locations for power settings where photos were not available.[‡]

* It is assumed that $\gamma = 1.3$ for the burn-through flame.

† A photo of the flame for the 70 percent power setting was not clear enough to accurately define the shock locations.

‡ One method of extrapolating the results of Fig. 1 to higher engine pressure ratios is to (1) use the results of Ref. 3 to determine the location of the first shock, and (2) extrapolate the curves for shocks 2, 3 and 4 parallel to the curve for shock 1.

Flat Plate Normal Shock Corrections: In a supersonic flow, there is a difference between the impingement pressure on a flat plate and the pressure recorded by a pitot probe at the same location--because the normal shock will be farther from the plate than from the probe (see Fig. 2). Thus, the probe will experience a pressure* consistent with the Mach number at the probe location (M_{probe}) while the plate pressure will be consistent with a Mach number upstream of the plate location (M_{plate}). This effect has been observed experimentally by Snedeker and Donaldson² (see Fig. 39 of Ref. 2). In addition to the above effect, the shock in front of the plate may coalesce with the shock in the jet, giving rise to a different shock structure than would exist if no plate were present.

Because of these effects the first step in interpreting the fiat plate pressure data was to "convert" these readings to equivalent pitot probe pressures; i. e., the pressure downstream of a normal shock at the local Mach number. This was done by utilizing the photos in Ref. 2, which show shock detachment distances for a flat plate located at various positions in a jet. By interpreting the pitot probe data of Ref. 2 in terms of local Mach numbers, the curve shown in Fig. 3 was constructed. This figure was used in the following way to determine equivalent pitot probe pressures in the burn-through flame:

1. From the flat plate pressure[†] (Table 2) and free stream stagnation pressure[‡] (i. e., upstream of the normal shock) a free stream Mach number was computed (from standard normal shock tables⁴).

2. From Fig. 3, the shock detachment distance was determined. This fixed the point in the flow having the free stream Mach number found in 1, and therefore fixed the pitot pressures[§] at that point.

From the above procedure, pitot pressures were determined as a function of distance from the burn-through hole. These are plotted in Fig. 4, which will be discussed in more detail in the following section (Mach Number and Pressure Distributions).

* It is noted that both probe and plate pressures are stagnation pressures downstream of a normal shock, but at Mach numbers M_{probe} and M_{plate} , respectively.

† All flat plate pressures could not be used because of probable interference with the jet shocks at certain locations. Pressure data not considered valid are noted in Table 2.

‡ These computations will be discussed in the following section (Mach Number and Pressure Distributions).

§ It is noted that pitot pressure is defined as the stagnation pressure downstream of a normal shock in front of a pitot probe.

Mach Number and Pressure Distributions: The following procedure was used to determine the Mach number and pressure distributions:

1. The shock locations* were determined from Fig. 1.
2. Between the burn-through hole and the first shock, the pitot pressures and Mach numbers were determined using the method described under Flat Plate Normal Shock Corrections, with the free stream stagnation pressure equal to the chamber pressure.†
3. Conditions immediately downstream of the first shock (and all succeeding shocks) were determined by assuming the Mach number equals unity‡ behind the shock(s).
4. From the stagnation pressure downstream of the shock (from 3 above) and the pitot pressures (corrected flat plate pressures) the Mach number distribution between the first and second shocks was determined (similar to step 2.)
5. Static pressures were determined from Ref. 4, knowing the local Mach numbers and stagnation pressures, assuming $\gamma = 1.3$.§
6. The above procedure was repeated until the computed stagnation pressure loss across the shocks was not sufficient to account for the measured flat plate pressures. The stagnation pressure vs. distance curve downstream of this point was approximated as described in the following sample calculation.

* For the 50 percent and 60 percent power settings, there should be no shocks in the burn-through flame (see Table 1); the flow is completely subsonic.

† There are no stagnation pressure losses (along the centerline) before the first shock.

‡ This is a reasonable assumption since the Mach number behind the shock is approximately equal to or less than the jet exit Mach number (M_{ex}). Since the observed shocks are oblique, the downstream Mach numbers cannot be less than unity. Thus $M_2^{(0)} = 1$ was chosen to interpret these data.

§ Specific heat ratios should increase towards 1.4 with increasing distances from the burn-through hole as ambient air mixes with the combustion gases. However, for the range of Mach numbers under consideration, the effect upon the flame properties is negligible.

Results of calculations using the above procedure are given in Figs. 4a-4h. A detailed example for the 95 percent power setting follows:

Before First Shock

- $P_0 = 4.5$ atm (from Table 1)
- at $x = 1$ in., $P_{0FP} = 3.0$ atm (from Table 2)
- From Ref. 4, for $\gamma = 1.3$; $\frac{P_{0FP}}{P_0} = 0.67$, gives $M = 2.05$
- From Fig. 3, $\Delta/d = 0.25$
- $M_{\infty} = 2.05$ is then located at $x = 0.75$ in. (see Fig. 4a)
- From Ref. 4, $p/P_0 = 0.12$, thus $p = 0.54$ atm
- The Mach number curve is faired through three points; $M_{ex} = 1$ at $x = 0$, and 2 points ($x = 0.75$ and 1.2 in.) determined in the above manner.

At First Shock

- From $M_1^{(0)} = 2.3$ (from the faired Mach Number curve) and $M_2^{(0)} = 1.0$, the stagnation pressure downstream of the oblique shock is determined (from Ref. 5); $P_{O_2} = 3.8$ atm.
- From Ref. 5, a shock angle of 58° is found for this pressure loss. The following table gives a comparison of first-shock angles determined by the above method and those measured from the photos of Ref. 1.

<u>Engine Power Setting, Percent RPM</u>	<u>Shock Angle, deg.</u>	
	<u>Predicted</u>	<u>Measured</u>
90	60	52
30	64	58

This good agreement between the predicted and measured shock angles gives additional confidence in the assumption of $M_2^{(0)} = 1.0$.

Before Second Shock

- $P_0 = 3.8$ atm (from above)
- at $x = 3$ in., $P_{0FP} = 2.5$ atm (from Table 2)
- From Ref. 4 for $\gamma = 1.3$; $\frac{P_{0FP}}{P_0} = 0.66$, gives $M_\infty = 2.07$
- From Fig. 3, $\Delta/d = 0.25$
- $M_\infty = 2.07$ is then located at $x = 2.75$ in.

This procedure is continued until the calculated stagnation pressure loss is not sufficient to account for the measured flat plate pressure.* At the 95 percent power setting this condition occurs between the third and fourth shock. The stagnation pressure curve (Fig. 4a) is then continued by connecting the pitot pressures behind the 4th and 5th shocks (since $M_2^{(0)} = 1$, the stagnation pressure must equal the pitot pressure) and extrapolating the curve downstream of the 5th shock.

Velocity Distributions: Before local velocities can be computed the thermocouple readings must be corrected for radiation and conduction losses: these corrections were made (see Thermocouple Corrections for details), and the true gas stagnation temperatures are given in Fig. 4. The velocity is then computed from:

$$u = Ma \quad (1)$$

$$u = M \left[\gamma R \left(\frac{T}{T_0} \right) T_0 \right]^{1/2} \quad (1a)$$

where T/T_0 is a function of Mach number.⁴

* This is probably due to an increased stagnation pressure loss due to mixing between the ambient air and burn-through flame (see Influence of Mixing on Flame Properties). Because of the approximations in the present analysis and the inherent inaccuracies in the measured flat plate impingement pressures, this point cannot be determined with great precision.

Thermocouple Corrections

Radiation: Because of radiation from the thermocouple junction (and wires) to the surroundings, the equilibrium temperature of the junction, T_w is less than the true gas stagnation temperature, T_o . However, T_o can readily be determined by performing a heat balance (between convection to the junction and radiation from the junction). Assuming conduction along the wires is negligible* we get,

$$h(T_o - T_w) = \sigma \epsilon T_w^4 \quad (2)$$

Eq. (2) is used to solve for T_o , once the heat transfer coefficient, h , is known.

Heat Transfer Coefficient - There are no experimental data in the literature on heat transfer coefficients for hot, turbulent supersonic jets impinging on a flat plate. However, data are available for cold subsonic turbulent jets impinging on moderately heated flat plates,^{6,7} and a (well-confirmed) theoretical expression is available for stagnation point heat transfer in laminar flow.⁸ These pieces of information were combined in this study to obtain the local heat transfer coefficients.

Donaldson, et al.,⁶ compared their measured stagnation point heat transfer coefficients (for turbulent jets) with those computed from laminar stagnation point theory⁸ and showed that the ratio of the measured to calculated values is a function of distance from the jet exit (and not a function of Reynolds number). By extrapolating the data of Ref. 6, it was found that this ratio varied from about 1.1 to 1.5 for the range of x/d of interest in the present study. Thus the laminar stagnation point heat transfer coefficients were computed from the theory of Ref. 8, and all values were multiplied by an (average) factor of 1.3 to get the corresponding values of h for turbulent flow[†].

Values of h for laminar flow were computed from,⁸

$$Nu = \frac{hd}{k} = 0.66 Pr^{1/3} Re^{1/2} \left[\frac{d}{u} \left(\frac{du}{dy} \right)_0 \right]^{1/2}$$

The normalized velocity gradient; i. e., the term in square brackets, was measured by Snedeker and Donaldson² (for ratios of jet exit to ambient pressure from 1.0 to 3.5) to be about unity. It is important to note that, for

* This is shown under Conduction.

† Use of an average factor is consistent with the accuracy of this technique for calculating turbulent heat transfer coefficients.

supersonic flow, the local properties, u , ρ , etc., must be evaluated downstream of the normal shock in front of the plate. A sample calculation is given below, for the 80 percent power setting at $x/d = 2$.

- $M = 1.6$; $p_1 = 0.74$ atm (from Fig. 4d)
- $T_2/T_0 = 0.94$; $M_2 = 0.66$ (normal shock tables⁴)
- $T_0 = 3200^\circ\text{R}$ (Table 1); $T_2 = 3000^\circ\text{R}$
- $p_2 = 2.1$ atm $\left(\frac{p_2}{p_1} = 2.8$ from Ref. 4)
- $\rho_2^* = p_2/RT_2 = 0.027$ lb_m/ft³
- $u_2 = M_2 [\gamma RT_2]^{1/2} = 1700$ ft/sec
- $P_r^\dagger = 0.65$
- $\mu_2^\dagger = 3.5 \times 10^{-5}$ lb_m/ft-sec
- $Re = \frac{\rho_2 u_2 d}{\mu_2} = \frac{1}{12} \frac{(1700)(2.7)10^{-2}}{(3.5)10^{-5}} = 1.1 \times 10^5$
- $k^\ddagger = 0.06$ Btu/hr-ft-°R
- $h = 140$ Btu/hr-ft²-°R (from Eq. (3))

Using $h/h_{\text{turb}} = 1.3$ the value of h to be used for the radiation correction, is,

$$h_{\text{turb}} = 180 \text{ Btu/hr-ft}^2\text{-}^\circ\text{R}$$

A series of calculations was made to determine the range of h_{turb} for all values of x/d at all power settings. It was found that h_{turb} varied from approximately 160 to 200 Btu/hr-ft²-°R. Therefore, all subsequent calculations of the radiation correction used an average value[†] of $h_{\text{turb}} = 180$ Btu/hr-ft²-°R. Then using a value of $\epsilon = 0.2$ (Ref. 9) in Eq. (2), and the thermocouple

* Calculations of gas density utilize the gas constant for air, i. e., $R = 53.3$ ft-lb_f/lb_m-°R.

† Transport properties taken from Ref. 4, Table 2 (extrapolated).

‡ The use of an average value of h_{turb} (for all power settings) to compute the corrected stagnation temperatures is consistent with both the accuracy of this technique and the accuracy of the uncorrected flat plate thermocouple readings.¹

readings in Table 3 the actual gas stagnation temperatures were computed; these are listed in Table 4 and plotted in Fig. 4.

Smooth curves were drawn through the data in Fig. 4 and the faired values near the burn-through hole were used to estimate stagnation temperatures in the combustor for all power settings; these are listed in Table 1. Rust¹ reports that information furnished by the J-47 engine manufacturer (General Electric) indicates a maximum stagnation temperature in the combustor of 3500°R. In Table 1 it can be noted that this is exactly the stagnation temperature estimated for the 95 percent power setting. This good agreement implies that the thermocouple corrections are reasonable.

Conduction: Conduction from the thermocouple junction along the wires can influence the heat balance equation, Eq. (2), if the conductive heat transfer; i. e.,

$$q_{\text{cond}} = k_w A_w \left(\frac{dT}{ds} \right)_j \quad (4)$$

is not negligible compared to the convective heat transfer to the junction,

$$q_{\text{conv}} = h A_j (T_o - T_w) \quad (5)$$

Pertinent data on the thermocouple are:

- Material: Pt/Pt-13% Rh (Ref. 1)
- length to connectors = 10 in. (measured)
- $d_w = 0.02$ in. (measured)
- $k_w = 50 \frac{\text{Btu}}{\text{hr-ft-}^\circ\text{R}}$ (Ref. 19)
- junction (bead) diameter = 0.062 in. (measured)

As an example, the conductive heat transfer for a thermocouple reading of 3000°R, and an (assumed) temperature gradient* $(dt/ds)_j = 300^\circ\text{R/in.}$; i. e.,

* This assumed gradient is conservatively large since the junction and exposed wires are both subjected to the convective heating. This would make the temperature gradient at the junction much smaller than, in this case, 300°R/in., thereby reducing the conductive heat loss even further.

a linear gradient over the 10 in. length is

$$q_{\text{cond}} = 0.39 \text{ Btu/hr (Eq. 4)}$$

For $T_o = 3500^\circ\text{R}$, $T_w = 3000^\circ\text{R}$ and $h = 180 \text{ Btu/hr-ft}^2\text{-}^\circ\text{R}$, the convective heat transfer is

$$q_{\text{conv}} = 1.9 \text{ Btu/hr (Eq. 5)}$$

Thus, even using a conservatively large value of $(dT/ds)_j$, q_{cond} (for this case) is only 20 percent of q_{conv} . The conduction heat loss was found to be negligible for all test conditions, primarily due to a small wire diameter and relatively small temperature gradients along the wire.

Mass Flow Rates

Following determination of stagnation temperatures in the combustor, the mass flow rates can be computed via,

$$w = (p_{\text{ex}}/RT_{\text{ex}}) u_{\text{ex}} A_{\text{ex}} \quad (6)$$

Using the data given in Table 1, along with Eq. (6), gives the mass flow rates shown in Table 5.

Influence of Mixing on Flame Properties

Mixing between the burn-through flame and ambient air is the most important mechanism by which stagnation enthalpies in the flame decrease. Thus, a good measure of the effect of mixing on the flame properties along the centerline is the rate of decrease of stagnation enthalpy.* Nondimensional stagnation enthalpies (the usual manner of presenting high-temperature mixing data) are plotted in Fig. 5 for all power settings. An important parameter in the present study is the distance from the burn-through hole at which the effects of mixing are experienced on the flame centerline (the designated core region). The length of the core region, L , is arbitrarily defined as the value of x/d at

* Enthalpy is used as a mixing parameter rather than temperature because the specific heat of the flame varies over the temperature range of interest.

which $(H_o - H_{amb}) / (H_{o_c} - H_{amb}) = 0.95$. These core lengths are given in Table 6, together with the angle of spread of the mixing region,* i. e. $\tan^{-1} d/2L$.

In order to extrapolate these test results to other systems the core lengths are correlated with enthalpy flux at the burn-through hole, i. e.,

$$E = P_{ex} u_{ex} (H_{o_c} - H_{amb}) \quad (7)$$

for all power settings. (See Fig. 6). The data can be fitted reasonably well by a straight line if we neglect the point for the 50 percent power setting.

There are not much data available on high-temperature turbulent jets to compare with the results of the NAFEC tests. However, O'Connor, et al.,¹¹ have measured the axial variation of stagnation enthalpy† in turbulent jets of partially dissociated N_2 , with an enthalpy flux of about 5×10^4 Btu/ft²-sec. These data are shown in Fig. 5. We observe that the corresponding point on the core length vs. enthalpy flux curve (Fig. 6) is somewhat lower than the NAFEC data. This agreement is, however, good considering the uncertainties in estimating core lengths from the enthalpy data. The straight line correlation should be useful for determining core lengths and mixing region angles (cf. Table 6) for larger burn-through holes with greater mass flows. However it is unadvisable to use Fig. 6 to determine core lengths for high compression ratio (say, 12:1) engines, for which the burn-through jet boundaries are highly expanded. Because of this expansion, the core lengths should be greater than shown in Fig. 6, for a given enthalpy flux. Interpretation of highly underexpanded rocket plume data would be needed to get an equivalent correlation.

Some additional data‡ on stagnation temperature and enthalpy axial distributions in high temperature jets are given by Harsha.¹²

* Caution must be exercised in attempting to compare the results of Fig. 5 and Table 6 with corresponding data on high temperature jets issuing from a perfectly expanded, smoothly converging nozzle. It has been shown by Donaldson and Gray¹⁰ that the mixing rates are higher for jets emanating from a flat surface (which would be similar to combustor burn-throughs) than for the above-mentioned jets. This is due to the difference in air entrainment patterns.

† These data are for a jet (at a pressure of 1 atm) emanating from a flat plate. so they should compare reasonably well with the NAFEC data.

‡ There was insufficient time in the present study to interpret these data.

Suggested Experimental Methods for Future Test Programs

It is suggested that future test programs on higher compression ratio engines be designed to obtain data on local burn-through flame properties (temperature, pressure, etc.) and local heat transfer coefficients (for a geometry similar to that of a firewall material in the flame). In addition, analytical models which can be used to predict burn-through flame properties and heat transfer coefficients should be developed. After it has been demonstrated that predictions and test data are in good agreement, the models should be used to develop a set of design charts--giving heat transfer coefficients, stagnation temperatures and pressures as a function of axial and radial distance from the burn-through hole, for parametric variations of combustor stagnation pressure, temperature and hole sizes. These are the necessary input data for determining the response of firewall materials to these burn-through flames. It is important to note that the development of accurate analytical models will avoid the necessity of obtaining test data each time a new combustor is designed or an existing system is re-designed. These models are also necessary in order to design a standard flame (which simulates a combustor burn-through flame) to test firewall materials.

Specific measurements that should be taken in future test programs are listed below.

Burn-Through Flame Properties: (These should be taken as a function of axial and radial distance from the burn-through hole at a sufficient number of points to define the properties within each shock cell)

1. Pressure - Both pitot and static pressure tubes should be used to record both the stagnation pressure behind a normal shock and the local static pressure (cf. Refs. 13 and 14). These data are then used to determine local Mach numbers.

2. Stagnation Temperature - A stagnation point thermocouple should be used, with provisions made to minimize heat conduction errors (cf. Ref. 15). This can be accomplished by using very small lead wires and inserting the junction far enough into the flame so that the junction and wires are at about the same temperature.

Photographs: These are especially important for determining the flame boundaries and shock structure--for comparison with analytical predictions. Color photos are useful for estimating the extent of the mixing region--but black and white photos are sufficient for defining the shock structure.

Sampling: It would be very useful to know the composition of the burn-through flame--particularly to determine if any unburned fuel escapes the combustor. The fuel could (subsequently) react with ambient air giving higher flame temperatures than would otherwise be expected. Gas samples should be taken via a sampling probe throughout the burn-through jet (in the core and mixing regions). Samples taken at the burn-through hole will indicate how much unburned fuel is available to react with ambient air. A detailed discussion of the problems involved in gas sampling and the considerations involved in designing sampling probes are given in Ref. 16.

Effects of Noncircular Holes: Since a burn-through hole will probably not be circular in practice, it is important to test the influence of, for example, an elliptical hole with jagged edges, on flame properties. Significant differences between test results on circular and noncircular holes must then be accounted for in predicting actual burn-through flame properties.

Heat Transfer Coefficients: These can be determined by measuring local heat transfer rates and wall temperatures for a flat plate (simulating a firewall material) normal to the burn-through flame. (The plate impingement pressures should also be recorded as a function of radial distance from the plate stagnation point since these are the actual pressures experienced by firewalls.) Two possible nonsteady-state methods of measuring heat transfer coefficients are:

1. Calorimeter Discs (see, e. g. Ref. 6) - In this technique the temperature-time response of a uniform temperature disc is recorded. The heat transfer is computed from,

$$q_{\text{conv}} = m_D c_p D \left(\frac{dT_w}{dt} \right)_{t=0} \quad (8)$$

then

$$h = \frac{q_{\text{conv}}}{T_0 - T_w} \quad (9)$$

where T_0 is the measured stagnation temperature.

2. One-Dimensional Plug - A cylindrical plug is inserted in the flat plate, with one end exposed to the gas. The surface is insulated over its length and temperature of the exposed end is measured as a function of time. From the solution to the heat conduction equation for a one-dimensional semi-infinite

rod* with a convective boundary condition, and the measured temperature of the exposed end, the heat transfer coefficient can be determined from,

$$\frac{T_p - T_i}{T_o - T_i} = 1 - \exp\left[\left(\frac{h}{k_p}\right)^2 \alpha t\right] \operatorname{erfc}\left(\frac{h}{k_p} \sqrt{\alpha t}\right) \quad (10)$$

Additional information on this technique is given in Ref. 18.

-
- * The plug acts as a semi-infinite rod because data are taken before the temperature of the back end can increase.

CONCLUSION

Based on the results of this study program, it is concluded that:

The computed pressures, temperatures and mass flows reported herein closely define the environment experienced by any material encountering a combustor burn-through flame from an engine operating within the pressure range specified in this report.

APPENDIX A

FIGURES EVOLVING FROM THE STUDY OF TEST DATA
ON JET ENGINE COMBUSTOR BURN-THROUGH FLAMES

ENGINE POWER SETTING, % rpm

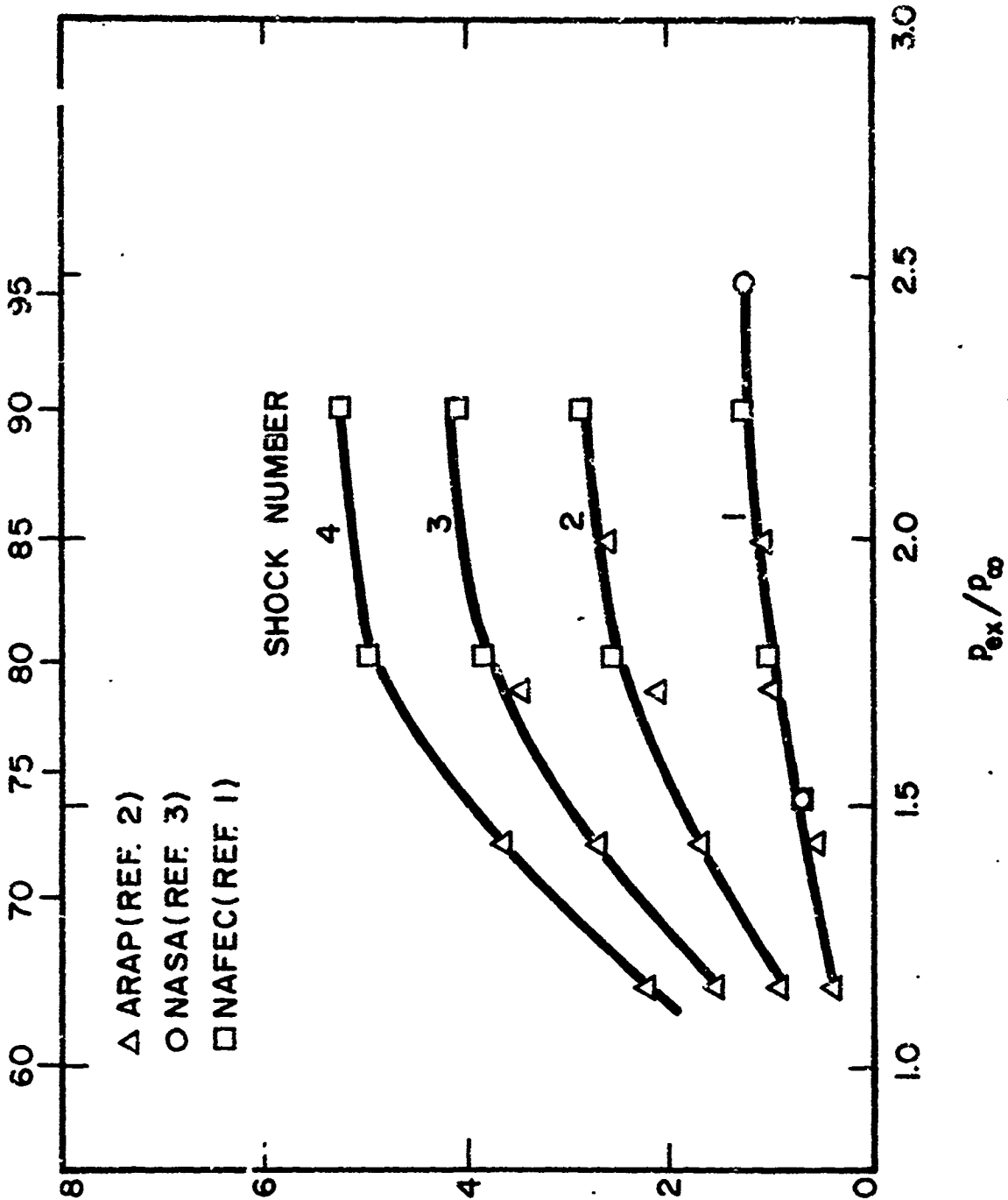


FIG. 1 COMPARISON BETWEEN SHOCK LOCATIONS IN NAFEC TESTS AND UNDEREXPANDED AIR JET DATA

DISTANCE FROM BURN-THROUGH HOLE, x/d

Preceding page blank

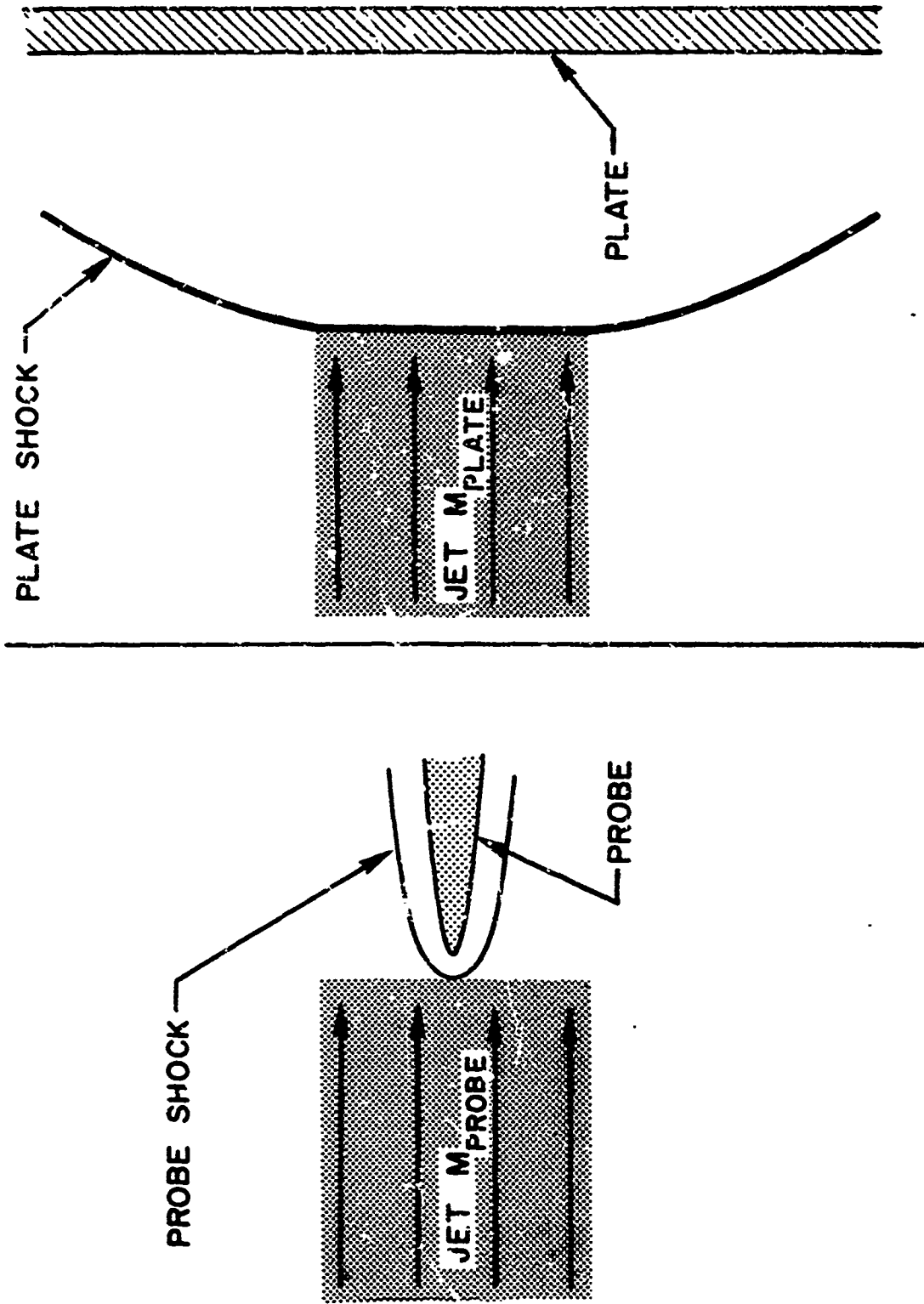
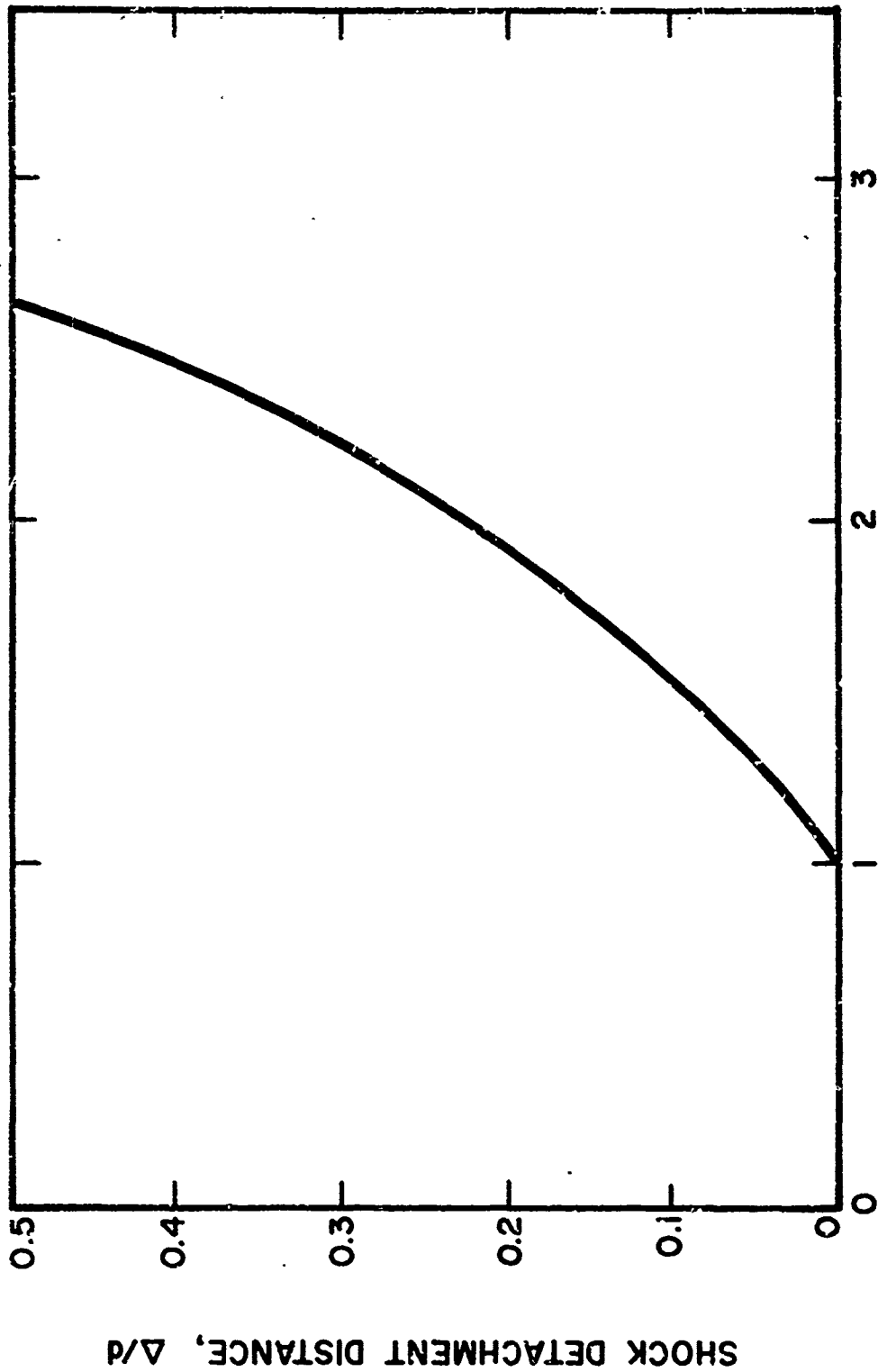


FIG. 2 RELATIVE POSITIONS OF SHOCKS UPSTREAM OF A FLAT PLATE AND A PITOT TUBE



MACH NUMBER BEFORE NORMAL SHOCK, M_1

FIG. 3 EFFECT OF MACH NUMBER ON SHOCK DETACHMENT DISTANCE FROM FLAT PLATE

Interpreted from data of Snedeker and Donaldson.²

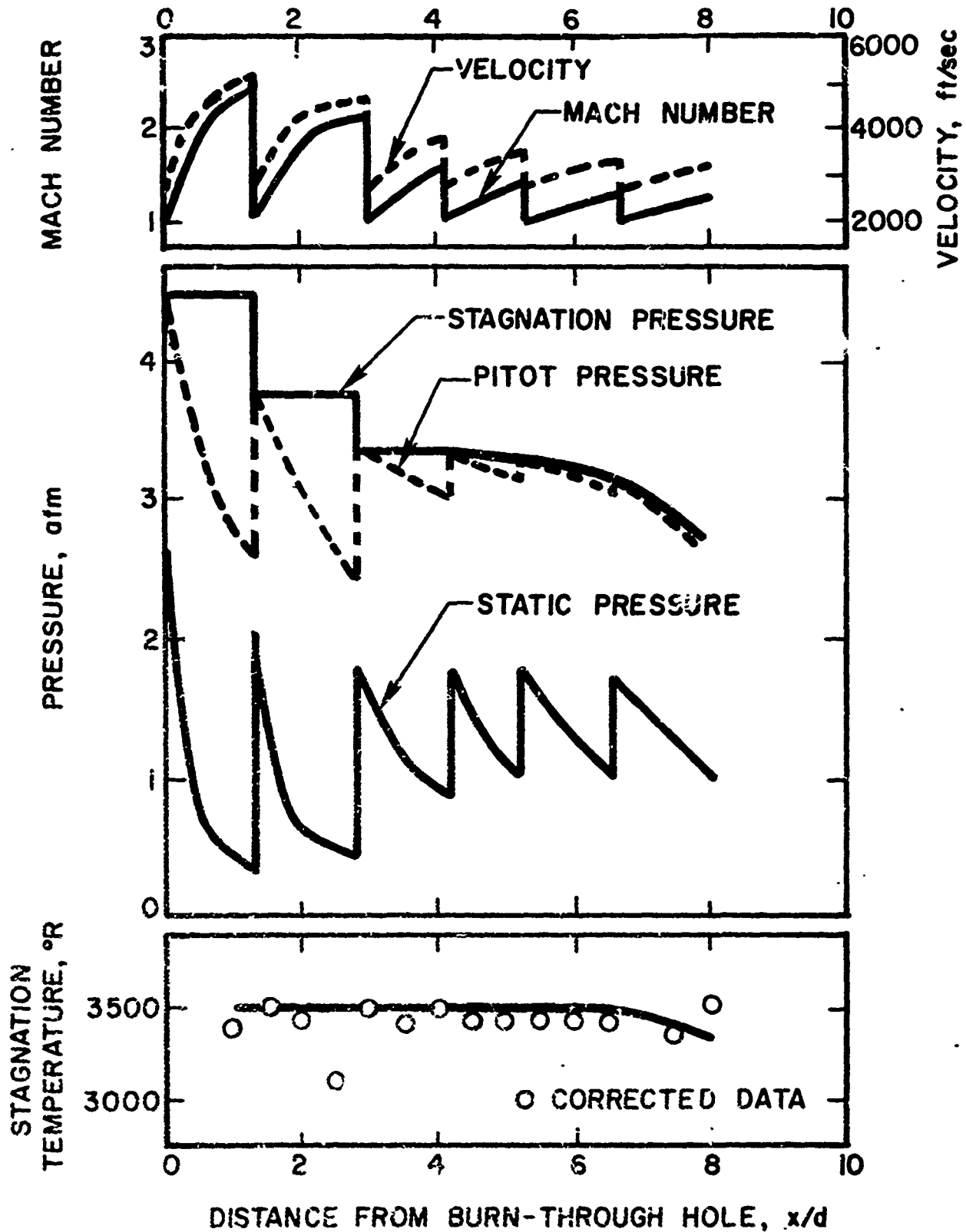


FIG. 4a PROPERTY DISTRIBUTIONS ALONG CENTERLINE OF BURN-THROUGH FLAME

95% power setting

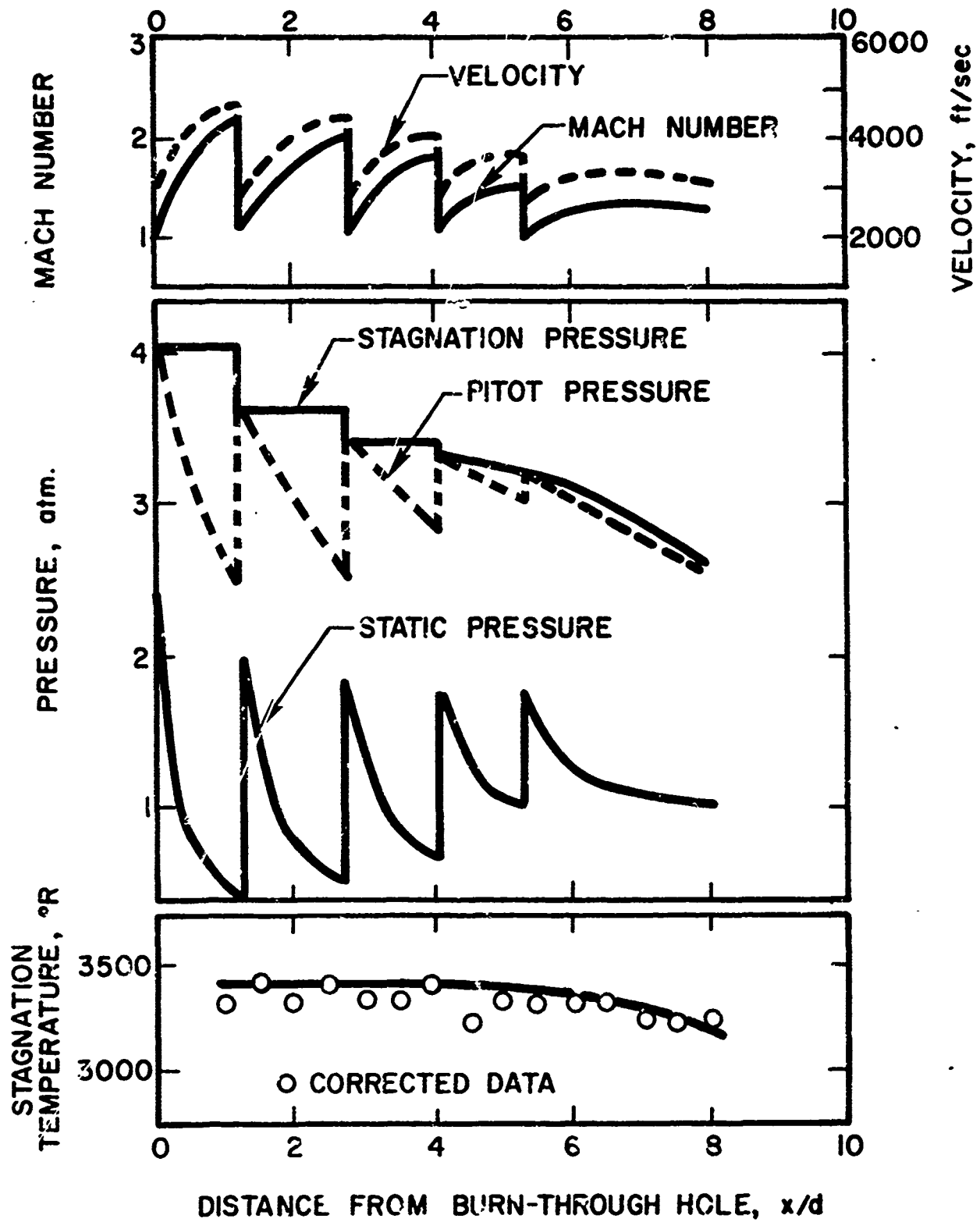


FIG. 4L PROPERTY DISTRIBUTIONS ALONG CENTERLINE OF BURN-THROUGH FLAME

90% power setting

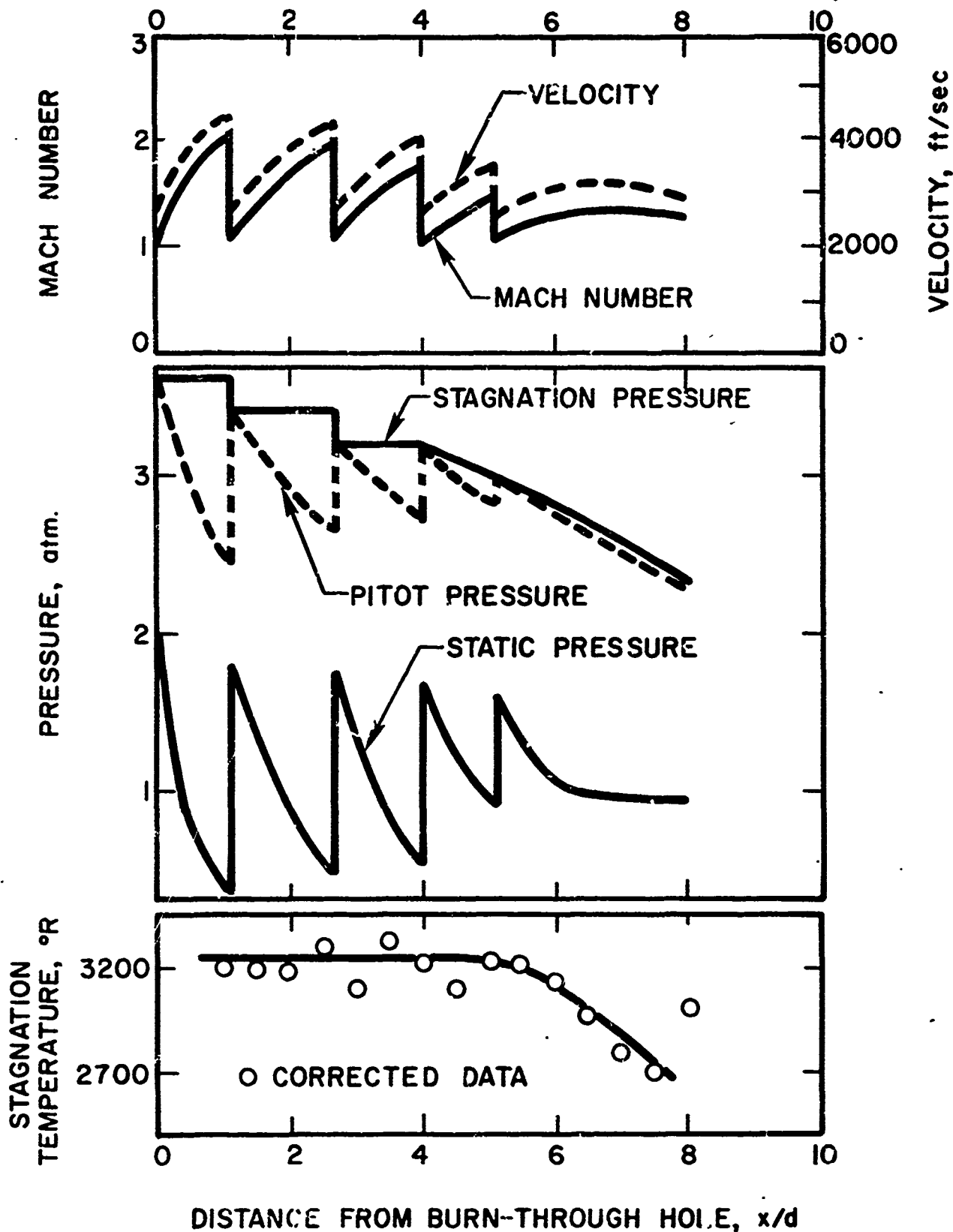


FIG. 4c PROPERTY DISTRIBUTIONS ALONG CENTERLINE OF BURN-THROUGH FLAME

85% power setting
1-8

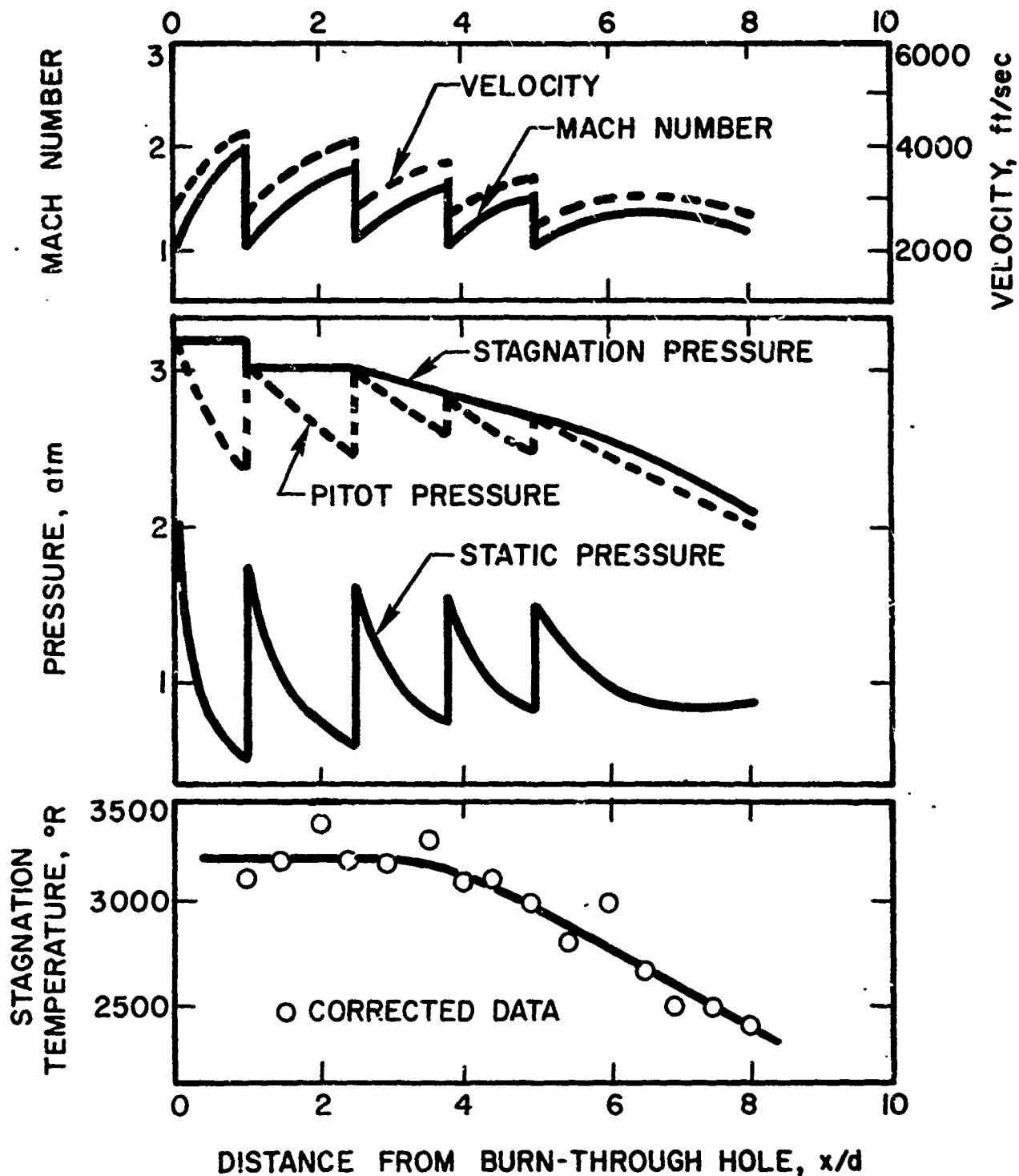


FIG. 4d PROPERTY DISTRIBUTIONS ALONG CENTERLINE OF BURN-THROUGH FLAME

80% power setting

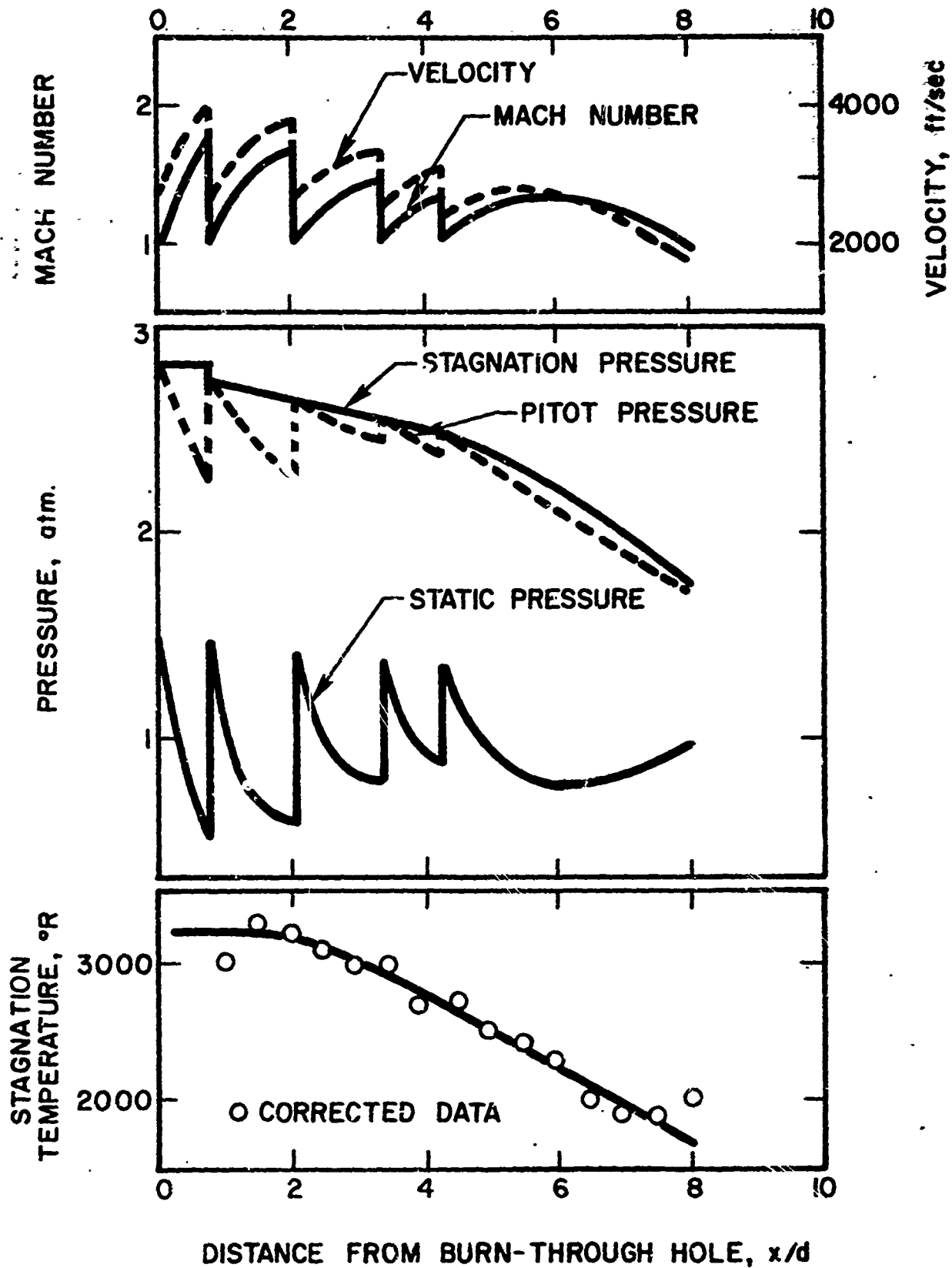


FIG. 4e PROPERTY DISTRIBUTIONS ALONG CENTERLINE OF BURN-THROUGH FLAME

75% power setting

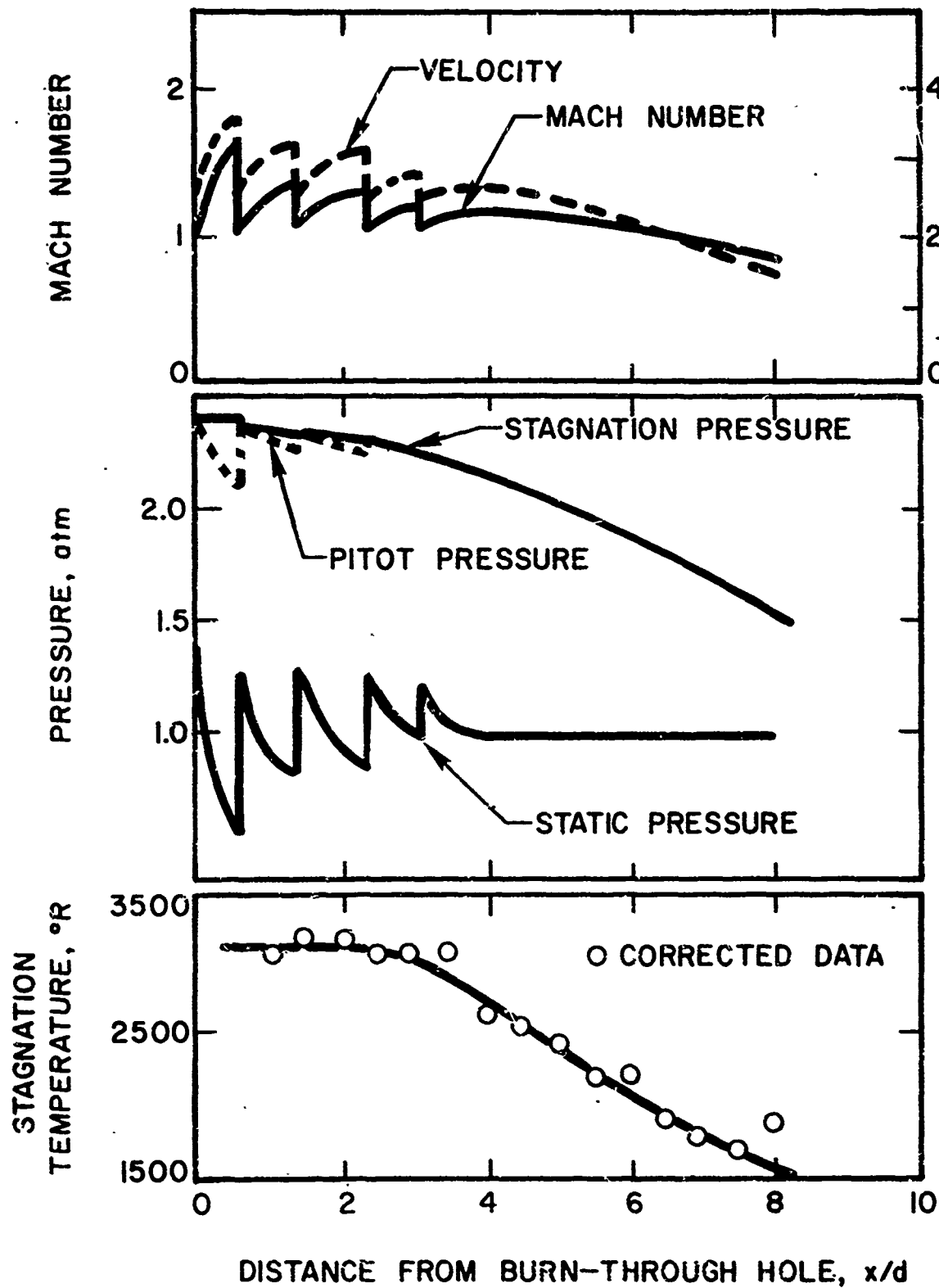


FIG. 4: PROPERTY DISTRIBUTIONS ALONG CENTERLINE OF BURN-THROUGH FLAME

70% power setting

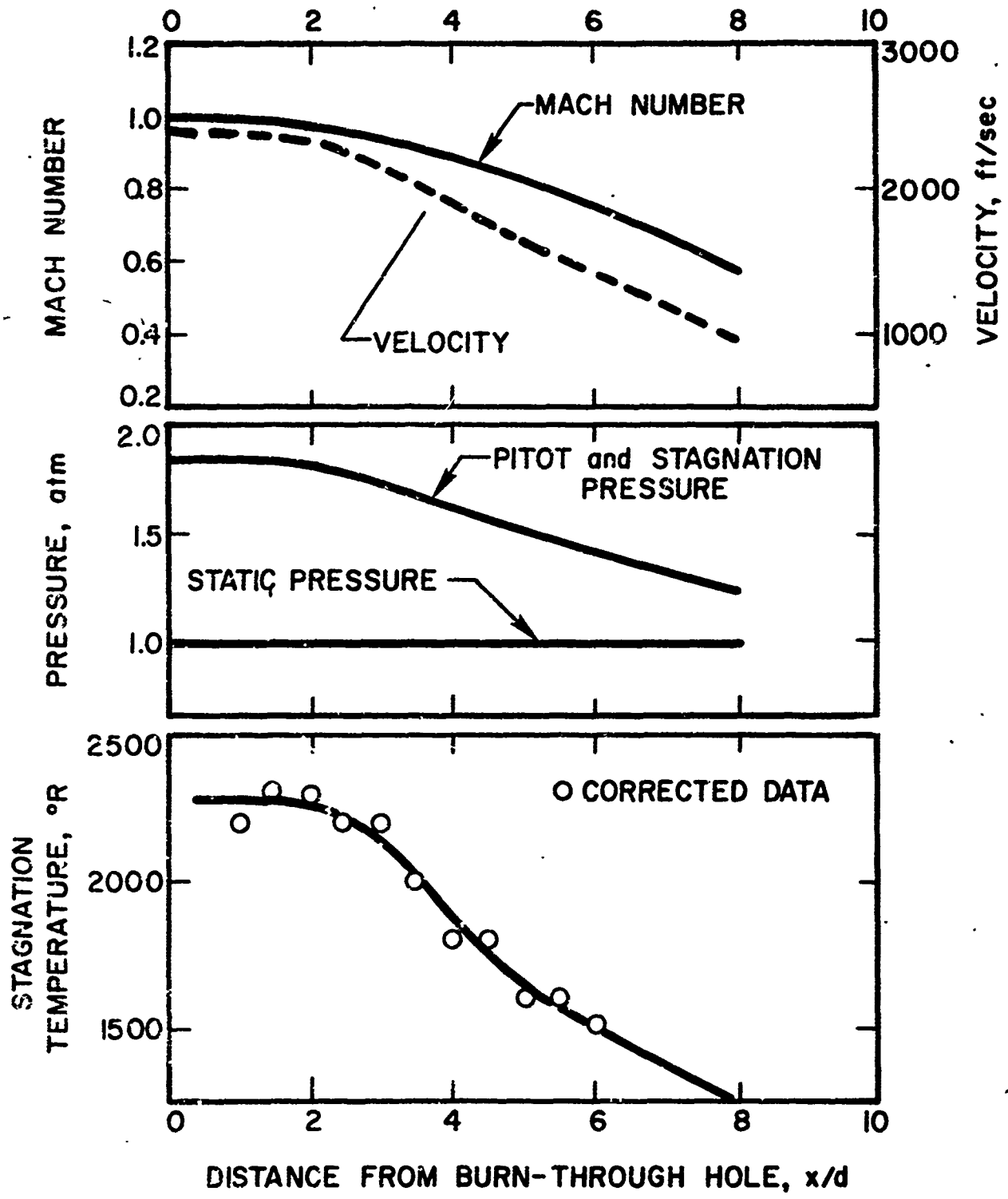


FIG. 4g PROPERTY DISTRIBUTIONS ALONG CENTERLINE OF BURN-THROUGH FLAME

60% power setting

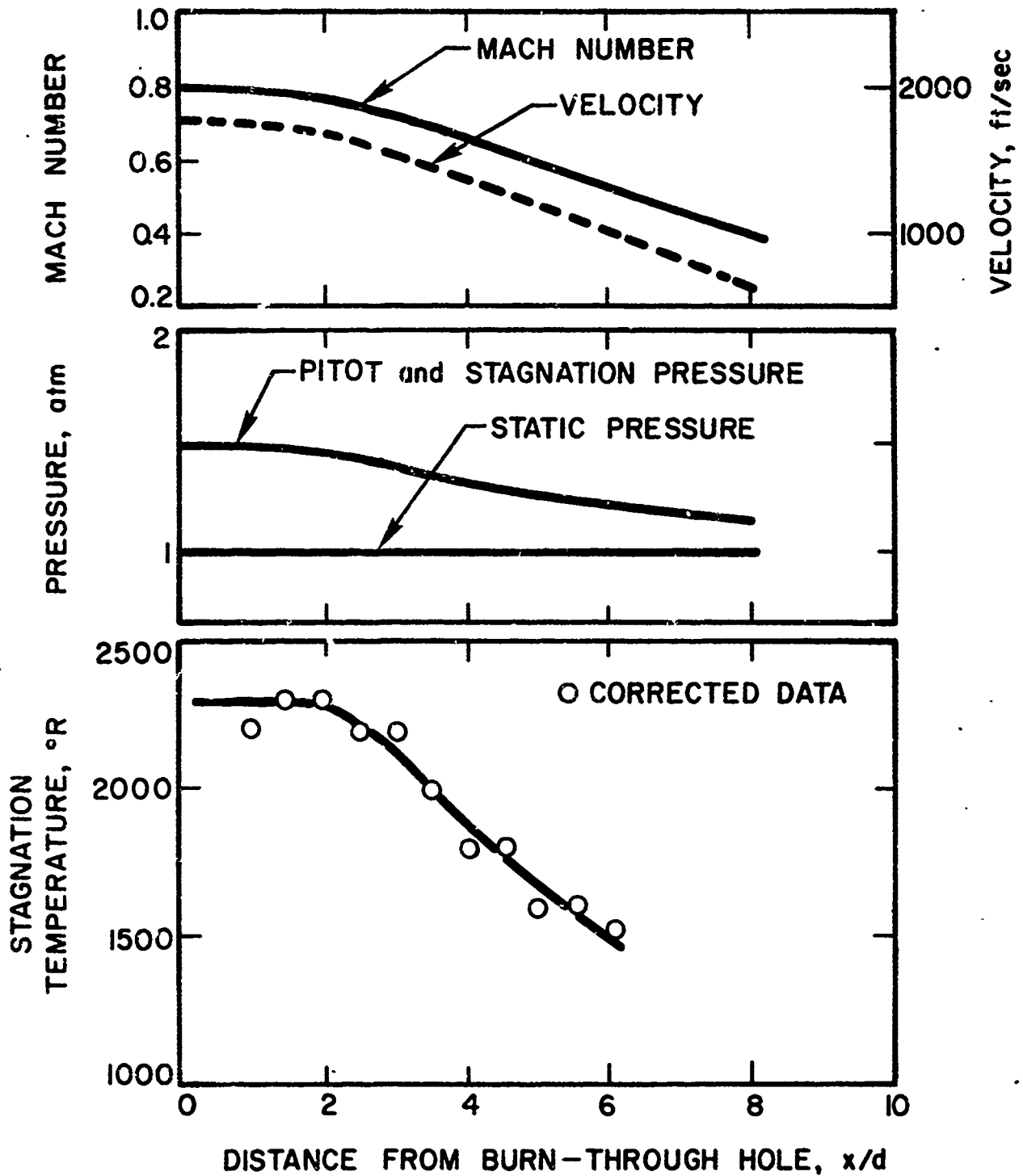


FIG. 4h PROPERTY DISTRIBUTIONS ALONG CENTERLINE OF BURN-THROUGH FLAME

50% power setting

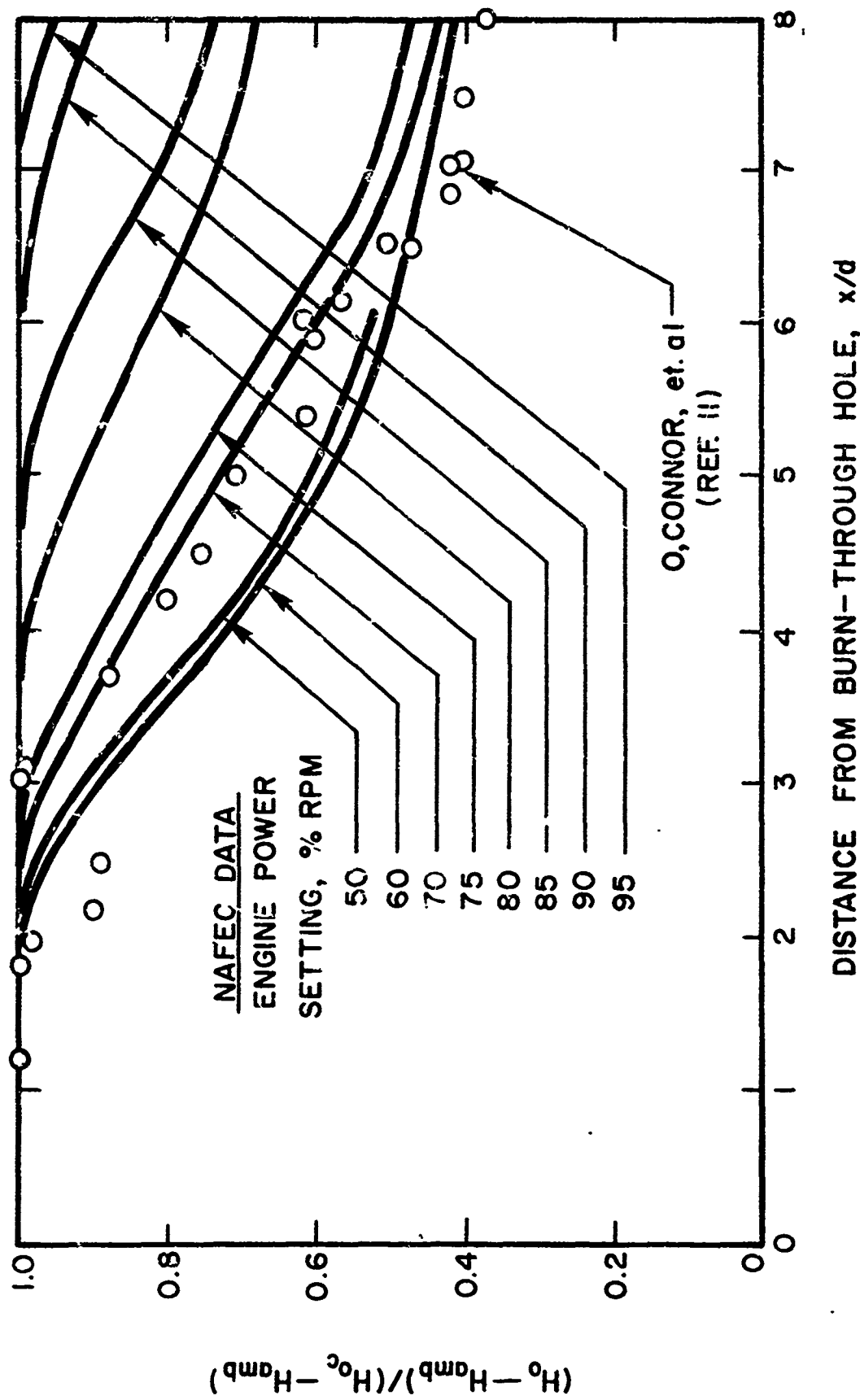


FIG. 5 EFFECT OF ENGINE POWER SETTING
 ON CENTERLINE STAGNATION ENTHALPY DISTRIBUTIONS

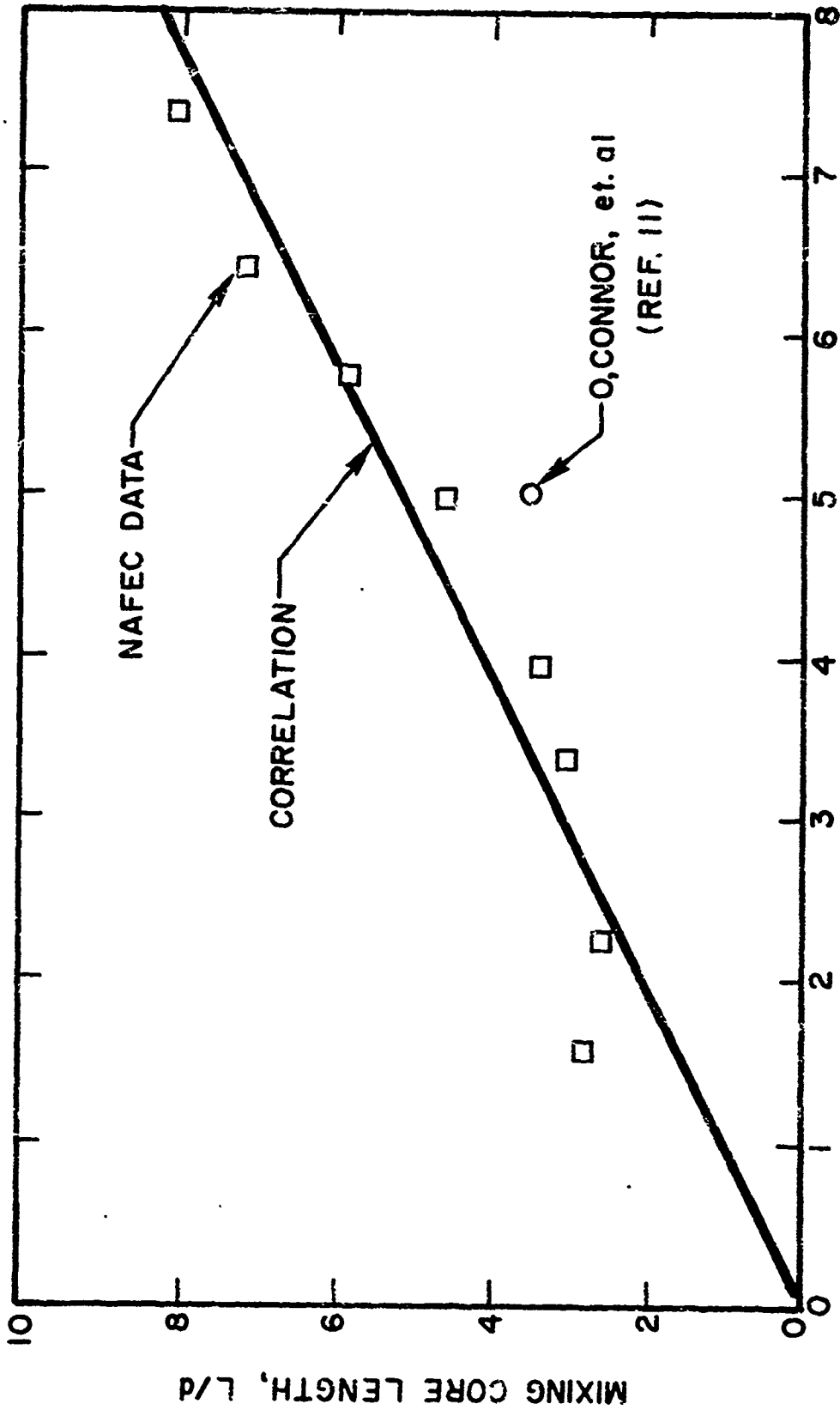


FIG. 6 INFLUENCE OF BURN-THROUGH FLAME ENTHALPY FLUX ON MIXING CORE LENGTH

Correlation developed for ratios of jet exit to ambient pressures ≤ 2.5

APPENDIX B

TABLES PERTINENT TO THE STUDY OF TEST DATA
ON JET ENGINE COMBUSTOR BURN-THROUGH FLAMES

TABLE i-PROPERTIES IN COMBUSTOR

<u>Engine Power Setting (% RPM)</u>	<u>Stagnation Pressure^a (atm)</u>	<u>Stagnation Temperature^b (°R)</u>	<u>Static Pressure at Hole^c (atm)</u>	<u>Velocity at Hole^e (ft/sec)</u>
50	1.5	2300	1.0 ^d	1800 ^d
60	1.8	2600	1.0	2400
70	2.4	3000	1.3	2600
75	2.8	3100	1.5	2600
80	3.2	3200	1.8	2700
85	3.6	3300	2.0	2700
90	4.1	3400	2.2	2800
95	4.5	3500	2.5	2800

a Taken from Ref. 1.

b Interpreted from thermocouple data corrected for radiation and conduction losses (see Fig. 4).

c From isentropic flow tables (Ref. 4); $\gamma = 1.3$.

d $M_{ex} \approx 0.8$. $M_{ex} = 1.0$ for all other power settings.

e From Eq. (1a) using $\gamma = 1.3$ and $R = 53.3 \text{ ft-lb}_f/\text{lb}_m\text{-}^\circ\text{R}$.

TABLE 2- FLAT PLAT IMPINGEMENT PRESSURES^a

Engine Power Setting (% RPM)	Distance from Burn-Through Hole, x/d														
	1	1.5	2	2.5	3	3.5	4	4.5	5	5.5	6	6.5	7	7.5	8
50	1.5	1.4	1.5	1.4	1.4	1.3	1.3	1.3	1.2	1.2	1.2	1.2	1.2	1.1	1.1
60	1.6	1.6	1.8	1.8	1.7	1.7	1.7	1.5	1.5	1.4	1.4	1.4	1.3	1.3	1.2
70	2.0	2.3	2.3	2.3	2.3	2.2	2.2	2.1	2.1	1.9	1.9	1.9	1.7	1.6	1.5
75	2.3	2.4	2.6 ^b	2.5	2.5	2.5	2.4	2.4	2.4	2.2	2.2	2.1	1.8	1.8	1.8
80	2.5	2.2 ^b	2.9 ^b	2.5	2.8	2.7	2.6 ^b	2.6	2.7 ^b	2.5	2.5	2.4	2.2	2.1	2.3
85	2.6	2.3	1.9 ^b	2.8	2.4 ^b	3.1	2.7	2.8 ^b	2.9	2.9	2.8	2.7	2.5	2.4	2.3
90	2.8	2.5	2.0 ^b	2.8	2.5	2.3 ^b	3.2	2.6 ^b	2.8 ^b	3.0	3.0	2.9	2.7	2.7	2.5
95	3.0	2.6	2.1 ^b	1.6 ^b	2.5	2.2 ^b	3.1	2.9 ^b	2.6 ^b	3.3	3.1 ^b	3.1	2.8 ^b	2.9	2.7

a Data taken from Ref. 1; rounded to 2 figures.

b Data not used in determining local Mach numbers (see Flat Plate Normal Shock Corrections).

TABLE 3-UNCORRECTED FLAT PLAT THERMOCOUPLE READINGS^a

Engine Power Setting (% F.P.M.)	Distance from Burn Through Hole, x/d								Temperature, °R						
	1	1.5	2	2.5	3	3.5	4	4.5		5	5.5	6	6.5	7	7.5
50	2100	2200	2200	2100	2100	2000	1800	1800	1600	1600	1500	b	b	b	b
60	2500	2500	2600	2400	2200	2200	2100	1900	1800	1600	1600	1600	1500	1500	1600
70	2800	2900	2900	2800	2800	2800	2500	2400	2300	2100	2100	1900	1800	1700	1900
75	2800	3100	3000	2900	2800	2800	2600	2600	2400	2300	2200	2000	1900	1900	2000
80	2900	3000	3200	3000	3000	3100	2900	2900	2800	2700	2800	2600	2400	2400	2300
85	3000	3000	3000	3100	2900	3100	3000	2900	3000	3000	2900	2800	2700	2600	2800
90	3100	3200	3100	3200	3100	3100	3200	3000	3100	3100	3100	3100	3000	3000	3000
95	3100	3300	3200	3000	3300	3200	3300	3200	3200	3200	3200	3200	3100	3000	3000

a Data taken from Ref. 1; rounded to 2 figures.

b Readings less than 1500°R.

TABLE 4- STAGNATION TEMPERATURES ON BURN-THROUGH FLAME CENTERLINE^a

Engine Power Setting (% RPM)	Distance from Burn-Through Hole, x/d														
	1	1.5	2	2.5	3	3.5	4	4.5	5	5.5	6	6.5	7	7.5	8
50	2200	2300	2300	2200	2200	2000	1800	1800	1600	1600	1600	1500	b	b	b
60	2600	2600	2700	2500	2300	2300	2200	1900	1800	1600	1600	1600	1600	1500	1600
70	3000	3100	3100	3000	3000	3000	2600	2500	2400	2200	2200	1900	1900	1700	1900
75	3000	3300	3200	3100	3000	3000	2700	2700	2500	2400	2300	2000	1900	1900	2000
80	3100	3200	3400	3200	3200	3300	3100	3100	3000	2800	2800	2700	2500	2500	2400
85	3200	3200	3200	3300	3100	3300	3200	3100	3200	3200	3100	3000	2800	2700	3000
90	3300	3400	3300	3400	3300	3300	3400	3200	3300	3300	3300	3300	3200	3200	3200
95	3300	3500	3400	3200	3500	3400	3500	3400	3400	3400	3400	3400	3300	3300	3400

^a Radiation and conduction corrections to thermocouple readings included; all numbers rounded to 2 figures.
^b Readings less than 1500°R

TABLE 5- MASS FLOW RATES

<u>Engine Power Setting</u> <u>(% RPM)</u>	<u>Mass Flow Rate^a</u> <u>(lb_m/sec)</u>
50	0.18
60	0.23
70	0.28
75	0.31
80	0.38
85	0.42
90	0.45
95	0.49

a From Eq. (6), using $\gamma = 1.3$ and
 $R = 53.3 \text{ ft-lbf/lb}_m\text{-}^\circ\text{R}$

TABLE 6-LENGTH OF CORE REGION

<u>Engine Power Setting</u> <u>(% RPM)</u>	<u>Length of Core Region, L</u> <u>(x/d)</u>	<u>Mixing Region Angle</u> <u>($\tan^{-1} d/2L$, deg)</u>
50	2.8	10
60	2.6	11
70	3.1	9.1
75	3.4	8.4
80	4.6	6.2
85	5.8	4.9
90	7.2	4.0
95	8.0	3.6

REFERENCES

1. Rust, T., "Investigation of Jet Engine Combustion Chamber Burn-Through-Fire," Final Report, Report No. FAA-RD-70-68, March 1971.
2. Snedeker, R.S. and Donaldson, C. duP., "Experiments on Free and Impinging Underexpanded Jets from a Convergent Nozzle," Aeronautical Research Associates of Princeton, Report No. ARAP-63, DDC AD 461 622, September 1964.
3. Love, E.S., Grigsby, C.E., Lee, L.P. and Woodling, M.J., "Experimental and Theoretical Studies of Axisymmetric Free Jets," NASA TR R-6, 1959.
4. Keenan, J.H. and Kaye, J., Gas Tables (John Wiley and Sons, New York, 1956).
5. Turner, M., "Compressible Flow Charts for Specific Heat Ratios From 1.18 to 1.40," Lockheed Missiles and Space Company, TM-53-14-96, September 1959.
6. Donaldson, C. duP., Snedeker, R.S. and Margolis, D.P., "A Study of Free Jet Impingement. Part 2. Free Jet Turbulent Structure and Impingement Heat Transfer," J. Fluid Mechanics **45** (Part 3), 477-512 (1971).
7. Huang, G.C., "Investigations of Heat Transfer Coefficients for Air Flow Through Round Jets Impinging Normal to a Heat Transfer Surface," J. Heat Transfer **85**, 237-245 (1963).
8. Dorrance, W.H., Viscous Hypersonic Flow (McGraw-Hill, New York, 1962).
9. Clayton, W.A., "A 500° to 4500°F Thermal Radiation Test Facility for Transparent Materials," Measurement of Thermal Radiation Properties of Solids (NASA SP-31, Washington, 1963), pp. 445-460.
10. Donaldson, C. duP. and Gray, K.E., "Theoretical and Experimental Investigation of the Compressible Free Mixing of Two Dissimilar Gases," AIAA J. **4**, 2017-2025 (1966).
11. O'Connor, T.J., Comfort, E.H. and Cass, L.A., "Turbulent Mixing of an Axisymmetric Jet of Partially Dissociated Nitrogen with Ambient Air," AIAA J. **4**, 2026-2031 (1966).

12. Harsha, P. T., "Free Turbulent Mixing: A Critical Evaluation of Theory and Experiment," AEDC-TR-71-36, February 1971.
13. Howarth, L. (ed.), Modern Developments in Fluid Dynamics - High Speed Flow, Vol. II (Clarendon Press, Oxford, 1956), Chap. XI.
14. Ladenburg, R. (ed.), Physical Measurements in Gas Dynamics and Combustion (Princeton University Press, Princeton, 1954), Chap. B.
15. Ibid., Chap. D.
16. Tiné, G., Gas Sampling and Chemical Analysis in Combustion Processes (Pergamon Press, New York, 1961).
17. Schneider, P. J., Conduction Heat Transfer (Addison-Wesley, Cambridge, 1955).
18. Cresci, R. J. and Libby, P. A., "Some Heat Conduction Solutions Involved in Transient Heat Transfer Measurements," WADC TN 57-236, ASTIA AD 130 800, September 1957.
19. Weast, R. C. (ed.), CRC Handbook of Chemistry and Physics - 49 Edition (Chemical Rubber Company, Cleveland, 1968).